Quantum Electronics **47** (7) 620–626 (2017)

ACTIVE ELEMENTS

https://doi.org/10.1070/QEL16370

Gain distribution in the volume of a solid-state active element of a diode-pumped high-power laser

T.I. Gushchik, A.E. Drakin, N.V. D'yachkov, V.V. Romanov

Abstract. **We propose a technique for calculating the spatial gain profile in the volume of a solid active element of a high-energy laser pumped by laser diode arrays, which takes into account the properties of the radiation pattern of semiconductor lasers. This technique is employed to calculate the profile of the gain in a neodymium glass active element. By the example of a rod of rectangular section 4.5 by 4.5 by 25 cm we show that, by varying the pump system parameters, it is possible to define the profile of the gain: for instance, a profile uniform over the cross section (with its nonuniformity under 2.5%), with a peak at the centre or in peripheral regions, with a specific energy deposition of ~1 J cm^{-3}.**

Keywords: *solid-state laser active element, diode pumping, control of gain profile.*

1. Introduction

Diode-pumped solid-state lasers have firmly occupied a prominent place among variously designed low- and medium-power lasers. In this case, the kilowatt cw power level with these lasers was reached even 10 years ago [1–5] and is not something extraordinary nowadays. As to lasers with a high pulsed power and a pulse energy of the order of several tens of joules and above 100 J, today there exists a highly limited number of such facilities [6–9]. Intensive research is pursued in this area and major projects are also contemplated (see, for instance, Refs [10, 11]). The replacement of lamp pumping with diode pumping is not only energetically advantageous but also offers additional useful possibilities. One of them consists in the formation of the desired stored energy distribution and thereby of the optical gain in an active element.

The problem of producing the desired spatial gain profile is directly related to the problem of optical beam profiling. We note that the use of modern chirped pulse amplification (CPA) technology [12] of optical pulse stretching–compression in the amplification of high-power optical fluxes is highly sensitive to the optical nonlinearity, which results in the variation of phase relations for the optical harmonics under amplification. The variations in intensity and population inversion over the cross section of the active element may also lead to undesirable changes in these phase relations due to the optical nonlinearity. This nonlinearity may not only be of the Kerr type but may also be caused by anomalous dispersion, which is due to gain saturation and is always inherently present in the amplifying medium. This nonlinearity was first considered in Ref. [13]. It is responsible for self-phase modulation in the radiation amplification both in a semiconductor active medium (see, for instance, Refs [14, 15]) and in solid-state active media (see, for instance, Refs [16, 17]). This nonlinearity was included in the simulation of a petawatt laser in Ref. [18].

In the long run the spatial nonuniformity of the population inversion and intensity may limit the ultimate attainable duration of optical pulses at the output of the amplifier system. In this connection the formation of the desired spatial profile is among the problems that are solved by using diode pumping in high-power laser facilities. An example is provided by Ref. [6], where the use of computer-controlled diode pumping made it possible to implement the spatial gain distribution in the form of a fourth-order super-Gaussian with an accuracy of 2%, which corresponded to the desired transverse distribution of optical beam intensity.

However, the advantages of diode pumping consist not only in the convenient formation of the desired spatial distribution of the population inversion (gain). Equally important is the higher pulse-to-pulse reproducibility of its parameters in comparison with flashlamp pumping. Any system intended for correcting (controlling) the phase shifts of the harmonics that participate in short-pulse formation, for instance acousto-optic modulators [19, 20], may operate only under conditions of sufficiently high reproducibility and with the possibility to precisely control the spatial distribution of the population inversion in the active element. In this respect a laser diode source of pump radiation is known to be advantageous over any discharge radiation source, including flashlamps.

At the same time we have to observe that diode pumping, despite all its advantages, has not yet found wide use in high-power laser facilities. The reason lies with only one though highly significant circumstance: its high cost in comparison with flashlamp pumping.

It is therefore clear that the practical implementation of such a facility should be preceded by its sufficiently reliable simulation. There is good reason to this in order to understand to what extent the expenses for the facility construction are justified by the potential benefits for its parameters. This aspect of research is present to one or other extent in all developments of diode-pumped laser facilities. For instance, by

T.I. Gushchik, A.E. Drakin, N.V. D'yachkov P.N. Lebedev Physical Institute, Russian Academy of Sciences, Leninsky prosp. 53, 119991 Moscow, Russia; e-mail: gushchik@lebedev.ru, dyachkov@lebedev.ru, drakin@lebedev.ru;
V.V. Romanov Russian Federal Nuclear Centre 'All-Russian Research Institute of Experimental Physics', prosp. Mira, 37, 607188 Sarov, Nizhnii Novgorod region, Russia

Received 23 March 2017; revision received 19 May 2017
Kvantovaya Elektronika **47** (7) 620–626 (2017)
Translated by E.N. Ragozin

numerical simulations alone it is possible to select the optimal absorption coefficient of the active material as some compromise between different tendencies exhibited in the variation of absorptivity. It is evident that lowering the absorptivity improves the uniformity and, at the same time, decreases the pump efficiency. In turn, the lowering of pump efficiency unambiguously makes the facility more expensive with retention of the stored energy level.

Some simulation results of the spatial gain distribution in diode-laser-pumped active elements with the stored energy of several hundred joules were published in Refs [21, 22]. However, the technique of obtaining these results is either based on particular-case codes or is applicable to the active elements of specific shape, since there is no general description of the optical model for the geometry of radiation propagation from laser-diode emitters to the active element.

This work was undertaken to somewhat fill this gap and construct an optical model of a laser-diode illuminator (a laser head) for calculating the spatial gain distribution (population inversion) in a rod-shaped active element with the inclusion of the radiation pattern of laser-diode emitters, the properties of the active element, and the possibility to store energy at a level of several hundred joules. Of special interest are the calculated data concerning the optimisation of the uniformity of the spatial gain distribution and the pumping efficiency for a Nd-glass rod of rectangular section as the most promising version of an active element for a high-power laser facility which harnesses the optical pulse stretching–compression technology.

It is clear that the same model may be used for a similar calculation for rods of other parametrically similar laser media like Yb:fluoride-phosphate glass, Yb:CaF_2, Yb:YAG, etc.

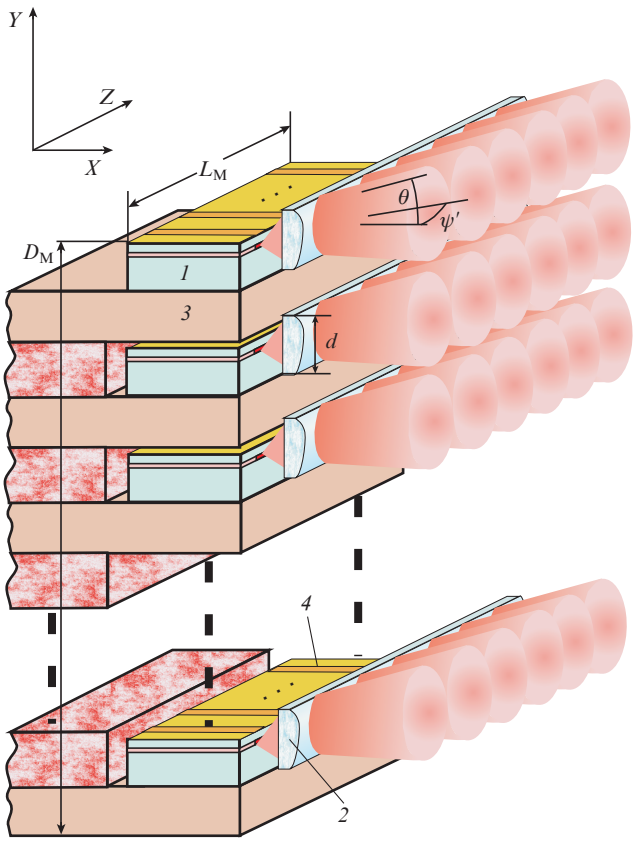

Figure 1. Typical structure of a laser-diode matrix: (*1*) laser-diode linear arrays; (*2*) cylindrical microlens for collimating the radiation in the plane perpendicular to heterostructure layers; (*3*) metallised ceramic plate for heat removal; (*4*) strip contact of an individual laser diode. Matrix dimension: $D_M \times L_M$.

2. Method for gain profile simulations

Today a diode-laser matrix is considered as the most suitable construction element for the laser-diode pump system of a high-power laser. It is a two-dimensional array of independent diode lasers assembled in the form of a diode-laser line depicted schematically in Fig. 1. The line in its turn is a monocrystalline bar of a semiconductor heterostructure, for instance GaAd/AlGaAs, with more than ten technologically integrated separate diode lasers. This line may be considered as a linear array of laser diodes. A large number of linear arrays combined in one structure are a two-dimensional emitter array, which we consider as a laser-diode matrix. Each individual linear array of laser-diode emitters is additionally equipped with its own output cylindrical microlens.

The mutual arrangement geometry of the cylindrical microlens and the laser-diode array is such that the focal plane of the lens coincides with the output face of the laser-diode array. Therefore, the lens collimates the radiation in the XY plane and in doing this does not markedly change the angular beam divergence in the XZ plane. The employment of the microlens is caused by a significant initial diode-laser divergence ($\theta \approx 30°–50°$) in the XY plane due to the small transverse beam size (~1 μm or smaller) along the Y axis at the output laser mirror. However, owing to the single-mode wave amplitude distribution in this transverse direction (the so-called 'fast' axis perpendicular to heterostructure layers) the divergence was nevertheless diffraction-limited. That is why the beam divergence after the microlens may also be diffraction-limited, now at the lens aperture d. Since usually $d > 100$ μm, the divergence in the XY plane after the microlens would be expected to amount to a fraction of a degree. In the majority of cases the real divergence ranges between 0.5° and 5°. It is determined by the microlens quality and the accuracy of assembling the linear array and its coupled microlens.

The overall optical beam of the matrix is formed as the sum of individual beams of all lasers, whose axes are randomly deflected (due to microlens assembling tolerances) from the normal of the matrix mounting surface. Therefore, there is good reason to employ the normal distribution law for the dependence of radiation brightness B on the angle θ. The variance $\Delta\theta$ will be a variable parameter in our simulations, which characterises the fabrication accuracy of the diode matrix equipped with microlenses.

As for the optical beam divergence in the other direction at the microlens output, it corresponds to the radiation divergence of an individual diode laser. As regards this direction, high-power diode lasers operate, as a rule, by a large number of transverse modes. Nevertheless, for the majority of laser diodes the dependence of radiation brightness B on the angle ψ' is essentially nonzero only for angles $|\psi'| < 10°$. In most cases, 90% of the optical beam power is confined in this angular range.

We consider the version of optical diode pumping of the optical element depicted in Fig. 2. It shows the cross section of the illuminator and the active element in the plane perpendicular to its longitudinal axis. The laser-diode matrices are mounted in four similar segments, which symmetrically sur-

round the active element. Since the illuminators are similar and symmetric relative to each other, the pump intensity distribution produced by each illuminator is obtained by way of 90° rotation, in the corresponding direction, of the pump intensity distribution produced by the neighbouring illuminator. Each segment is the surface of a cylinder with the axis parallel to the axis of the active element. In the general case, the axis of each cylinder is displaced to one or other side by the same distance relative to the axis of the active element. The segment is assumed to be symmetric relative to the corresponding XZ [segments (*1*) and (*3*)] or YZ [segments (*2*) and (*4*)] planes, with the result that the pump intensity distribution is also symmetric relative to these planes. The space between the diode matrices and the active rod is 'closed' by highly reflecting corner (*5*) and end (not shown in Fig. 2) plane mirrors.

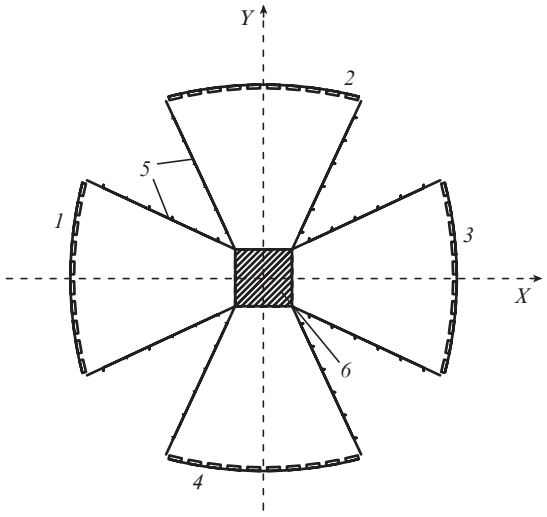

Figure 2. Simplified diagram of a diode-pumped laser head (the parameters of the active element and the matrix for this scheme are collected in Table 1): (*1–4*) diode matrix surfaces; (*5*) corner plane mirrors; (*6*) active element.

We will take advantage of the circumstance that the length L of the active element is far greater than its lateral dimension a ($L \gg a$). Furthermore, we restrict ourselves to the case when the brightness B of the illuminator emission is independent of the coordinate on the illuminator surface, i.e. all diode lasers in all matrices are equally pumped and produce on average the same power. This version of the scheme of diode pumping of the active rod, first, is most simple and easy for practical implementation and, second, permits numerical simulations to be greatly simplified by reducing the intricate three-dimensional problem to a simpler two-dimensional one.

The radiation of each laser has a relatively short coherence length and the lasers themselves are mutually incoherent, and so our treatment in the geometrical optics approximation will be quite adequate. In the framework of this approach, outside of the matrix the radiation power ΔI emanating from a surface area ΔS of the diode matrix into a solid angle $\Delta\Omega$ in the direction defined by the polar angle θ and the meridional angle ψ' (as shown in Fig. 1) is as follows:

$$\Delta I = B(\theta,\psi')\,\Delta S\Delta\Omega, \tag{1a}$$

where

$$B(\theta,\psi') = \left(\sum_{i\in\Delta S} I_i(\theta,\psi')\,\Delta\Omega\right)\Big/\Delta S; \tag{1b}$$

$\Delta\Omega = \cos\theta\Delta\theta\Delta\psi'$; $I_i(\theta,\psi')\Delta\Omega$ is the power of the ith diode laser emitted into a solid angle $\Delta\Omega$ in the direction defined by angles θ and ψ'; and ΔS is the element of the matrix surface. It will be assumed that element ΔS has dimensions which, on the one hand, are sufficiently small in comparison with the characteristic dimensions of the optical system elements: the matrix (D_M, L_M), the active rod (a, a, L), the distance between the matrix and the active rod, etc. On the other hand, they are large enough to contain a significant number of diode lasers which enter in the sum of equality (1b), so that this equality may be considered as the definition of function $B(\theta,\psi')$ – the angular brightness of illuminator emission.

Figure 3 shows schematically the path of a ray from the diode matrix, its refraction at the input face of the active element, and passage through the active element. Point A' corresponds to the point of intersection of the ray with the input face of the active element and point $A(x,y)$ corresponds to the point inside the active element with coordinates x, y; ψ', ψ and φ', φ are the meridional and polar angles outside and inside the active element, respectively. Parameter x_0 is the X-displacement of the centre of curvature of the illuminator (point O_c) from the centre of the active element (point O_{ae}, shown is the case $x_0 < 0$), θ is the angle between the incident ray and the local normal to the matrix surface, β is the angle of inclination of the matrix surface to the surface of the active element, Δ is the distance between the matrices, and θ_{sm} is the opening angle of the side illuminator mirrors. The refractive index outside of the active element is equal to unity and n is the refractive index of the active element itself. Then, the ray refraction at the face of the active element is described by the formulas

$$n\sin\varphi = \chi(\psi')\sin\varphi', \tag{2a}$$

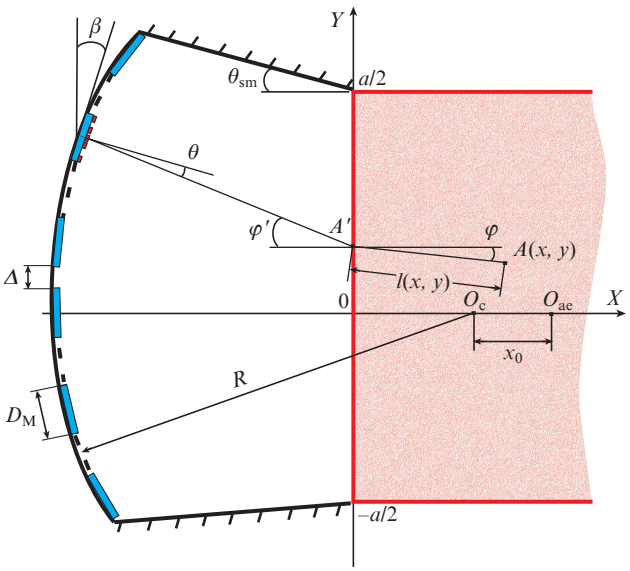

Figure 3. Part of the scheme of active element illumination by the system of diode matrices located on the cylindrical surface of radius R. The height of the cylinder segment (the dimension along the Z axis) is equal to the length of the active bar.

$$\chi(\psi') = \frac{\cos\psi'}{\left[1 - (\sin\psi'/n)^2\right]^{1/2}}. \quad (2b)$$

By analysing equality (2b) it is easy to show that the value of χ for $|\psi'| < 10°$ and $n = 1.59$ will differ from unity by no more than 1%, which is below the uncertainty to which the remaining parameters employed in the simulation are known. Therefore, without impairing the precision of our simulations we may go over to the two-dimensional problem and assume that $\chi(\psi') \equiv 1$ in equality (2a) and employ for the radiation brightness the integral of the function $B(\theta,\psi')$, which appears in Eqn (1), over all angles ψ'. In view of the above, the expression for the brightness may be written in the form

$$B(\theta) = B_0 \exp\left(-\frac{\theta^2}{2\Delta\theta^2}\right),$$

where

$$B_0 = P_0\left[\int_{-\pi/2}^{\pi/2} \cos\theta \exp\left(-\frac{\theta^2}{2\Delta\theta^2}\right)\mathrm{d}\theta\right]^{-1};$$

P_0 is the power density emitted by the matrix (the power radiated from a unit surface of the matrix in W cm^{-2}).

In accordance with the ray path from the matrix to point (x, y) inside the active bar plotted in Fig. 3, the power density P_a absorbed at this point is of the form:

$$P_a = \alpha B_0 \int_{\varphi\in\gamma} [1 - R(\varphi)]\exp[-\alpha l(x,y)] \times \exp\left[-\frac{\theta(\varphi)}{2\Delta\theta^2}\right] n\cos\varphi\,\mathrm{d}\varphi, \quad (3)$$

where α is the absorption coefficient; $\theta = (\varphi' - \beta)$ is the angle between the ray and the local normal to the matrix surface; φ' is the angle of ray incidence on the face of the active element from the side of the diode matrix; β is the angle between the plane of the matrix surface and the illuminated face of the active element; $R(\varphi)$ is the reflection coefficient at the face of the active element; γ is the interval of φ angles in which the diode matrices are seen from point x, y; and l is the optical path length of the ray in the active element.

The integral in expression (3) comprises all ray trajectories whose end is at a fixed point x, y and the other end intersects the plane of diode matrices at different points x', y', depending on the angle φ. These are the direct rays emanating directly from the matrices towards the surface of the active element as well as the rays reflected from the corner plane mirrors (*5*) in Fig. 2. Also included in expression (3) are the rays which experience total internal reflection from the side faces of the active element parallel to the XZ plane and find their way to point x, y.

With the knowledge of absorbed power density it is easy to find the stored energy density and the gain g:

$$E(x,y) = P_a(x,y) f(T) \xi, \quad (4)$$

$$g(x,y) = \frac{E(x,y)\sigma_L}{\hbar\omega_L}, \quad (5)$$

where $f(T)$ is the effective duration of the pump pulse; $\xi = \hbar\omega_L/(\hbar\omega_p)$ is the pump photon defect; $\hbar\omega_L$ is the photon energy of a laser transition of an ion; $\hbar\omega_p$ is the pump photon energy; and σ_L is the cross section for stimulated leaser transition. For a rectangular pump pulse of duration T, the effective pump duration

$$f(T) = \tau_s[1 - \exp(-T/\tau_s)], \quad (6)$$

where τ_s is the lifetime of the excited ion state of the active element.

The declared technique of calculating the spatial distribution of stored energy and gain over the cross section of the active element applies to the case when the pump is produced by one segment of the illuminator, as shown in Fig. 3. Similar calculations for pumping with two and four segments (Fig. 2) may be performed by taking into account the pumping scheme symmetry and summing the data obtained for one segment.

The nonuniformity of the spatial distribution of the gain was calculated as its rms deviation from the average value g according to the relations

$$\bar{g} = \frac{1}{a^2}\int \mathrm{d}x\mathrm{d}y g(x,y), \quad (7)$$

$$\frac{\delta g}{\bar{g}} = \frac{1}{\bar{g}}\left(\int \frac{|g(x,y) - \bar{g}|^2 \mathrm{d}x\mathrm{d}y}{a^2}\right)^{1/2}. \quad (8)$$

Furthermore, we found the geometrical pumping efficiency factor K, which was the fraction of total laser diode power P absorbed by the rod:

$$K = \frac{\int P_a(x,y)\,\mathrm{d}V}{P}. \quad (9)$$

3. Simulation results

Figures 4 and 5 show the data of simulations performed to optimise the gain $\alpha = \sigma N$ of the active medium, which may be realised by varying the active ion density N and the pump radiation wavelength λ_p [because of the spectral dependence of the absorption cross section σ (Fig. 4a)]. In our case, the optimisation was carried out by varying the wavelength. The spatial uniformity $\delta g/\bar{g}$ of the gain and the pump efficiency were the parameters under optimisation. The simulations were performed for an illuminator with four segments (see Fig. 2), whose dimensions and parameters are collected in Table 1 (illuminator 1).

The absorption coefficient varies from ~1.6 cm^{-1} to ~0.7 cm^{-1} when the wavelength λ_p varies from 875 to 884.5 nm (Fig. 4a). In this case, K varies only slightly (from 0.9 to 0.86), while the nonuniformity of the gain decreases several-fold: ~0.5 to 0.06 (Fig. 4b). The further lowering of the absorption coefficient from 0.7 cm^{-1} to ~0.2 cm^{-1} (λ_p varies from 884.5 to 900 nm) leads to a significant (to 0.56) lowering of the pumping efficiency K and to a increase in spatial nonuniformity by nearly a factor of four.

This indicates that the optimal absorption coefficient for the pump radiation is ~0.7 cm^{-1} when the rod of square section is pumped by illuminator 1 with parameters given in Table 1 and the pump is optimised for the degree of spatial nonuniformity of the gain. In this case, the spatial nonuniformity of the gain is $\delta g/\bar{g} \approx 0.06$ and the pumping efficiency is only slightly lower: $K \approx 0.86$.

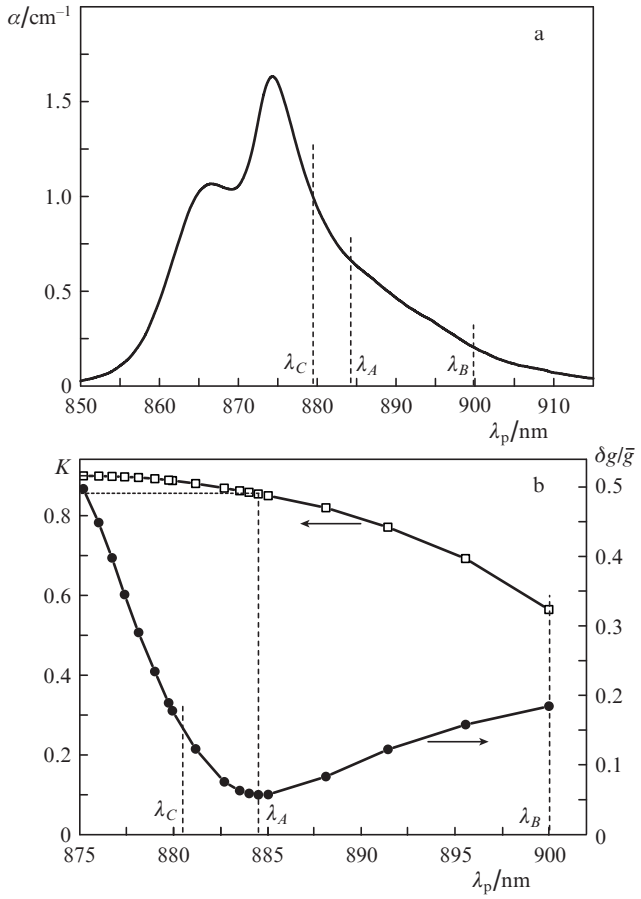

Figure 4. Pump-wavelength dependence of the absorption coefficient α in the active element on the $^4I_{9/2} - {}^4F_{3/2}$ transition of a Nd^{3+} ion in phosphate glass (the data of Ref. [23]) (a) and the pumping efficiency K, as well as of the relative nonuniformity $\delta g/\bar{g}$ of the spatial gain distribution for illuminator 1 from Table 1 (b).

Table 1.

Parameter	Illuminator 1	Illuminator 2
Active-element side length a	4.5 cm	4.5 cm
Illuminator's radius of curvature r	30 cm	45 cm
Displacement of the axis of cylindrical illuminator surface relative to the centre of the active element in the X axis, x_0	15 cm	−2 cm
Characteristic matrix size D_M	1.0 cm	1.0 cm
Distance Δ between matrix edges	0.56 cm	1.15 cm
Opening angle θ_{sm} of illuminator's side mirrors	25°	10.9°
Number of diode matrices in the illuminator arc	10	10
Diode matrix radiation intensity P_0	4 kW cm^{-2}	4 kW cm^{-2}
Directivity pattern width θ	5°	5°
Refractive index n of the active element	1.59	1.59
Neodymium ion density N	2×10^{20} cm^{-3}	2×10^{20} cm^{-3}
Laser wavelength λ_L	1.06 μm	1.06 μm
Pulse duration T	300 μs	300 μs
Excited state lifetime τ_s of active element ions	300 μs	300 μs
Effective pumping duration $f(T)$	192 μs	192 μs
Stimulated emission cross section σ_L of the laser level	3×10^{-20} cm^2	3×10^{-20} cm^2
Reflectivity of side mirrors	0.95	0.95
Optimal pump wavelengthи λ_A	884.5 nm	887.8 nm
Geometrical factor K of pumping efficiency	0.86	0.84
Spatial nonuniformity $\delta g/\bar{g}$ of the gain distribution	0.06	0.025
Pump photon defect ξ	0.834	0.838
Net pumping efficiency η	45.1%	44.2%

Desired in some cases for the purpose of correction is, by contrast, a nonuniform distribution of the gain, for instance a distribution with a peak at the centre or at some distance from the centre of the cross section of the active element. This may also be realised by varying the absorption coefficient due to variations of the pump radiation wavelength. This is testified by the data of Fig. 5, which shows the spatial profile of the gain distribution for three pumping wavelengths (they are denoted as λ_A, λ_B and λ_C and are shown on the wavelength scale in Fig. 4). These wavelengths correspond to the most uniform gain distribution (λ_A), the distribution with a central peak (λ_B), and the distribution with a maximum displaced from the centre of the element (λ_C).

The data of Figs 4 and 5 were obtained for the pumping by illuminator 1 (in the scheme of Fig. 2) with parameter values indicated in Table 1. In this illuminator, the axis of the cylindrical surface on which the diode matrices are located lies on the cylindrical surface of the opposite illuminating element (x_0 = 15 cm). In this case, the overall transverse illuminator dimension does not exceed ~30 cm and permit achieving the highest uniformity: $\delta g/\bar{g} \approx 0.06$. The spatial uniformity may be improved if the overall illuminator dimension is not limited. This possibility is demonstrated by Fig. 6, which depicts the data similar to those of Fig. 4 for an illuminator of larger size (illuminator 2 in Table 1). The minimal value of the $\delta g/\bar{g}$ curve in Fig. 6 is equal to ~0.025. For this illuminator geometry and the same characteristics of the matrices, increasing the illuminator size to ~90 cm is attended with an improvement in the uniformity of the gain distribution. Under this pumping, the specific stored energy is $E \approx 1$ J cm^{-3}. For an active element of length $L \approx 25$ cm the total stored energy will amount to ~500 J.

4. Discussion and conclusions

By the example of a diode-laser-pumped active rod of square section, in this work we demonstrated the possibility of controlling the gain distribution profile in the transverse direction to the optical axis. Although this possibility qualitatively is almost evident, quantitative characteristics, for instance the pumping efficiency and the degree of uniformity or, by contrast, the desired profile with a maximum on the optical axis could nevertheless be found by numerical simulations. This was done in our work by the example of pumping scheme simulations for an active element measuring 4.5 × 4.5 × 25 cm and a stored energy of several hundred joules. It is hoped that the simulations of this kind will permit simulating the parameters of the facilities under construction and thereby decreasing the number of expensive experimental research works.

Furthermore, we proposed and employed a technique for calculating the spatial gain profile of the active rod of a solid-state laser pumped by diode-laser matrices. The technique takes into account the formation of the directivity pattern

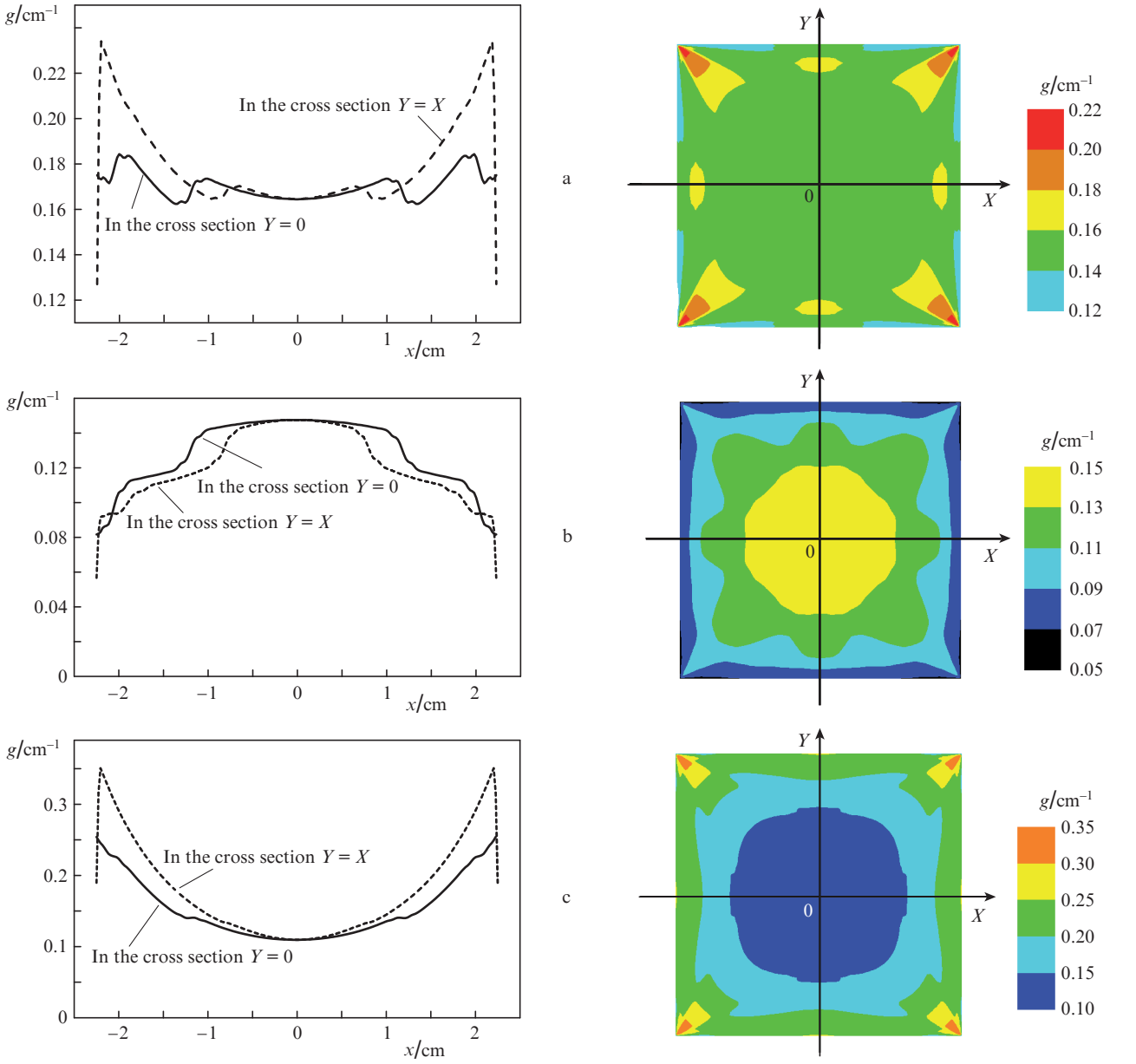

Figure 5. (Colour online) Gain distributions in the XY plane inside the rod for pumping radiation wavelengths $\lambda_A = 884.5$ nm (corresponds to the lowest nonuniformity of gain distribution $\delta g/\bar{g}$) (a), $\lambda_B = 900$ nm (b), and $\lambda_C = 879$ nm (c). Shown on the right are the corresponding two-dimensional gain distributions over the cross section of the active element.

(the angular brightness) of the total optical beam of a matrix from individual laser diode beams. The diode matrix itself is a convenient building element, since it comprises a large number of individual laser diodes and significantly simplifies the technology of making the pump system.

Although this technique was used to calculate the gain in one specific rod version, it may also be employed for the simulation of rods of other shape with different matrix arrangement geometry. Furthermore, in the calculation by formula (3) use was made of a constant brightness value, which corresponds to the same pumping current for all matrices. The brightness (the pumping current) may also be an additional factor for controlling the spatial gain profile. This all may be taken into account in the simulation in the framework of our technique by a non-essential change of the codes for the numerical calculation by formula (3).

The precision of the like simulations is known to be within the uncertainty due to the scatter of the initial optical and spectroscopic parameters of glasses of the same type. As shown in Refs [23, 24], the simulation accuracy of the output characteristics of diode-pumped neodymium-glass lasers is at a level of 10%. This gives grounds to believe that the accuracy of gain profile simulations performed in our work is also within this limit.

A high reproducibility of diode pump parameters and the capability of controlling the brightness of laser-diode matrices provide an additional possibility of controlling the gain profile without changing the optical configuration. With a feedback signal monitoring the real spatial gain profile on a specific facility it is possible to realise the automatic control of the real gain profile, or fitting it to the desired one. In this case, the accuracy may be defined by the precision of profile

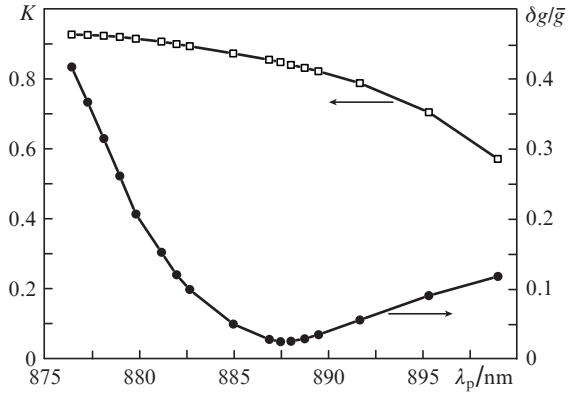

Figure 6. Geometrical pump efficiency factor K and spatial gain distribution $\delta g/\tilde{g}$ for illuminator 2 (Table 1) optimised for minimal $\delta g/\tilde{g}$ value as functions of the pumping wavelength λ_p.

control or the reproducibility of pump parameters and may be within several percent or better [6], as mentioned in the Introduction.

To summarise, we note that the diode pumping of high-power solid-state lasers may find wide use despite its high cost, because it is capable of providing additional characteristics and high performance of a laser facility, which is inherently impossible with the use of flashlamp pumping. For instance, the advantages of diode pumping may be realised in the construction of a small-size (table-top) petawatt laser harnessing the CPA stretching–compression technology for amplifying optical pulses.

References

1. Kravtsov N.V. *Quantum Electron.*, **31**, 661 (2001) [*Kvantovaya Elektron.*, **31**, 661 (2001)].
2. Grechin S.G., Nikolaev P.P. *Quantum Electron.*, **39**, 1 (2009) [*Kvantovaya Elektron.*, **39**, 1 (2009)].
3. Bruesselbach H., Sumida D.S. *IEEE J. Sel. Top. Quantum Electron.*, **11**, 600 (2005).
4. Pierre R.J.St., Mordaunt D.W., et al. *IEEE J. Sel. Top. Quantum Electron.*, **3**, 53 (1997).
5. McNaught St.S., Komine H., Weiss S.B., et al. https://doi.org/10.1364/CLEO.2009.CThA1.
6. Keppler S., Wandt C., Hornung M., et al. *Proc. SPIE*, **8780**, 87800I-1 (2013).
7. Lucianetti A., Novo T., Vincent B., et al. *Proc. SPIE*, **8080**, 80800N-1 (2011).
8. Lucianetti A., Divioky M., Sawicka M., Sikocinski P., Jambunathan V., et al. *Proc. SPIE*, **8602**, 860208-1 (2013).
9. Bowman S. *Opt. Eng.*, **52** (1012) (2013).
10. Bayramian A., Bopp R., Di Nicola J.M., Drouin M.A., Erlandson A., Fulkerson S., Jarboe J., Johnson G., Zhang H., et al. *OSA Techn. Digest (online)*, paper HT1B.5; LLNL-PROC-680089 (2016).
11. Mason P.D., Banerjee S., Ertel K., Phillips P.J., Butcher T., Smith J., De Vido M., Chekhlov O., Hernandez-Gomez C., Edwards C., Collier J. *Proc. SPIE*, **9893**, 989309 (2016).
12. Strickland D., Mourou G. *Opt. Commun.*, **56**, 219 (1985).
13. Javan A., Kelley P.L. *IEEE J. Quantum Electron.*, **2**, 470 (1966).
14. Bogatov A.P., Eliseev P.G., Sverdlov B.N. *IEEE J. Quantum Electron.*, **11**, 510 (1975).
15. D'yachkov N.V., Bogatov A.P., Gushchik T.I., Drakin A.E. *Quantum Electron.*, **44**, 997 (2014) [*Kvantovaya Elektron.*, **44**, 997 (2014)].
16. Antipov O.L., Bredikhin D.V., Eremeikin O.N., et al. *Quantum Electron.*, **36**, 418 (2006) [*Kvantovaya Elektron.*, **36**, 418 (2006)].
17. Gainov V.V., Ryabushkin O.A. *Quantum Electron.*, **41**, 809 (2011) [*Kvantovaya Elektron.*, **41**, 809 (2011)].
18. Filip C.V. https://doi.org/10.1364/CLEO_SI.2011.CTuJ5.
19. Chizhikov S.I., Garanin S.G., Goryachev L.V., Molchanov V.Y., Romanov V.V., Rukavishnikov N.N., Sokolovskii S.V., Voronich I.N., Yushkov K.B. *Laser Phys. Lett.*, **10**, 015301 (2013).
20. Molchanov V.Y., Romanov V.V., Rogozhnikov G.S., Yushkov K.B. *Opt. Lett.*, **41**, 5442 (2016).
21. Lapucci A., Giofini M. *Appl. Opt.*, **44**, 4388 (2005).
22. Siebold M., Podleska S., Hein J., et al. *Appl. Phys. B*, **81**, 615 (2005).
23. Bogatov A.P., Drakin A.E., Mikaelyan G.T., Miftakhutdinov D.R., Stadnichuk V.I., Starodub A.N. *Quantum Electron.*, **36**, 302 (2006) [*Kvantovaya Elektron.*, **36**, 302 (2006)].
24. Bogatov A.P., Drakin A.E., Miftakhutdinov D.R., Mikaelyan G.T., Starodub A.N. *Quantum Electron.*, **38**, 805 (2008) [*Kvantovaya Elektron.*, **38**, 805 (2008)].